

## NONLINEAR INTEGRAL EQUATIONS FOR SOLVING INVERSE BOUNDARY VALUE PROBLEMS FOR INCLUSIONS AND CRACKS

OLHA IVANYSHYN AND RAINER KRESS

Dedicated to Kendall Atkinson

**ABSTRACT.** For the problem to determine the shape of a perfectly conducting inclusion within a conducting homogeneous host medium from overdetermined Cauchy data on the accessible exterior boundary, that is, for an inverse Dirichlet boundary value problem, recently Kress and Rundell suggested a new inverse algorithm based on nonlinear integral equations arising from the reciprocity gap principle. The present paper extends this approach to the case of a perfectly insulating inclusion and the case of a perfectly conducting crack. The mathematical foundations of these extensions are provided and numerical examples illustrate the feasibility of the method.

**1. Introduction.** Inverse boundary value problems for the Laplace equation model electrostatic imaging methods in nondestructive testing and evaluation. Roughly speaking, in these applications an unknown inclusion within a conducting medium is assessed by imposing a voltage pattern at a number of electrodes attached to the boundary of the conducting object and measuring the resulting currents (or vice versa). For these inverse problems the reciprocity gap approach based on Green's integral theorem has been successfully applied, among others, by Andrieux and Ben Abda [6] for the identification of planar cracks and by Bryan et al. [9] for the reconstruction of cracks with unknown transmission conditions. For the problem to determine the shape of a perfectly conducting inclusion within a two-dimensional homogeneous host medium from overdetermined Cauchy data on the accessible exterior boundary, recently Kress and Rundell [20] suggested an inverse algorithm based on nonlinear integral equations arising from the reciprocity gap principle. The purpose of this paper is to extend this approach to the case of a perfectly insulating inclusion and the case of a perfectly conducting crack.

---

Received by the editors on May 23, 2005, and in revised form on July 26, 2005.

Let  $D$  be a doubly connected domain in  $\mathbf{R}^2$  with a smooth boundary  $\partial D$ , which consists of an interior boundary  $\Gamma_0$  and an exterior boundary  $\Gamma_1$ , such that  $\partial D = \Gamma_0 \cup \Gamma_1$  where  $\Gamma_0 \cap \Gamma_1 = \emptyset$ . By  $\nu$  we denote the unit normal to the boundary  $\partial D$  directed into the exterior of  $D$ . For convenience, we denote the bounded domain with boundary  $\Gamma_0$  by  $D_0$  and the unbounded domain with boundary  $\Gamma_1$  by  $D_1$ .

The electrostatic potential in an electrically conducting medium  $D$  containing a perfect insulator with boundary  $\Gamma_0$  is modeled by the following mixed boundary value problem: Given a function  $f \in H^{1/2}(\Gamma_1)$ , find a solution  $u \in H^1(D)$  of the Laplace equation

$$(1.1) \quad \Delta u = 0 \quad \text{in } D$$

that satisfies the mixed Neumann and Dirichlet boundary conditions

$$(1.2) \quad \frac{\partial u}{\partial \nu} = 0 \quad \text{on } \Gamma_0, \quad u = f \quad \text{on } \Gamma_1$$

in the sense of the trace theorem. It is well known that a unique solution exists to this mixed problem. For a classical approach via boundary integral equations we refer to [14] and for weak solutions to [18, 23]. For the approximate solution of the boundary integral equations plenty of techniques are available, among others we refer to [7, 18]. In the spirit of Atkinson, for our work we base the numerical solution on trigonometric polynomials. From Atkinson [7, p. 383], we quote: *It is the personal opinion of the author that the most efficient numerical methods for solving boundary integral equations on smooth planar boundaries are those based on trigonometric polynomial approximations, and such methods are sometimes called spectral methods. When calculations using piecewise polynomial approximations are compared with those using trigonometric polynomial approximations, the latter are almost always the more efficient.*

Assuming that the interior boundary degenerates into a crack  $\Gamma_c$ , that is, an open arc, the corresponding problem for a domain with a perfectly conducting crack is: Given a function  $f \in H^{1/2}(\Gamma_1)$ , find a solution  $u \in H^1(D)$  to the Laplace equation

$$(1.3) \quad \Delta u = 0 \quad \text{in } D$$

satisfying the Dirichlet boundary conditions

$$(1.4) \quad u = 0 \quad \text{on } \Gamma_0, \quad u = f \quad \text{on } \Gamma_1.$$

Again, existence and uniqueness of a solution to this crack problem are well established.

The topic of this paper is the inverse problem to determine the shape of the inclusion  $\Gamma_0$  or the crack  $\Gamma_c$  from an imposed voltage  $f$  on the outer boundary  $\Gamma_1$  and the measured currents

$$(1.5) \quad g = \frac{\partial u}{\partial \nu} \quad \text{on } \Gamma_1,$$

i.e., the resulting Neumann data. Note that in the case of the nonconducting inclusion by Green's integral theorem

$$(1.6) \quad \int_{\Gamma_1} g \, ds = 0$$

has to be satisfied as necessary condition for the total current. Concerning the issue of uniqueness the identifiability of the interior boundary curve  $\Gamma_0$  from one pair of Cauchy data  $(f, g)$  on the exterior boundary curve  $\Gamma_1$  for the case of a homogeneous Neumann condition on  $\Gamma_0$  can be reduced to the case of a homogeneous Dirichlet condition, see [15]. For the latter we refer to [18, 19] and note that the idea of the proof actually goes back to a private communication of Schiffer referenced in [22]. Addressing the ill-posedness of the inverse problem, among others, stability estimates were obtained in [2, 5, 8, 10, 12]. In these references, as a by-product, also the question of uniqueness is addressed.

For the inverse crack problem, in general, the shape of  $\Gamma_c$  is not uniquely determined by one pair of Cauchy data, since the crack might coincide with an equipotential line of the solution for the domain without crack. However, in [13] it was shown that two boundary measurements with appropriately chosen specific boundary voltages are sufficient to determine  $\Gamma_c$ . Stability for the crack reconstruction was considered in [1, 3, 4, 13].

For a harmonic function  $U \in H^1(D)$  we define the reciprocity gap functional

$$(1.7) \quad \mathcal{G}(U) := \int_{\Gamma_1} \left\{ f \frac{\partial U}{\partial \nu} - gU \right\} ds$$

in terms of the data  $f$  and  $g$ . Then, as a consequence of Green's second integral theorem, for the case of an insulating inclusion we have that

$$(1.8) \quad \mathcal{G}(U) = - \int_{\Gamma_0} p \frac{\partial U}{\partial \nu} ds,$$

where  $p := u|_{\Gamma_0}$  denotes the unknown Dirichlet boundary data on  $\Gamma_0$ . In the case of the domain with a crack, we obtain

$$(1.9) \quad \mathcal{G}(U) = \int_{\Gamma_c} hU ds,$$

where

$$(1.10) \quad h := \left. \frac{\partial u}{\partial \nu} \right|_+ - \left. \frac{\partial u}{\partial \nu} \right|_-$$

denotes the jump of the normal derivative across the crack  $\Gamma_c$ . Here,  $\nu$  is a continuous unit normal vector on  $\Gamma_c$ . By proceeding as in the classical proof of Green's representation formula for harmonic functions, see [18] it can be seen that (1.9), in addition to all  $U \in H^1(D)$ , is also valid for all  $U \in \text{span} \{ \Phi(x, \cdot) : x \in \Gamma_c \}$  where

$$(1.11) \quad \Phi(x, y) = \frac{1}{2\pi} \ln \frac{1}{|x - y|}, \quad x \neq y,$$

denotes the fundamental solution to the Laplace equation in two dimensions.

According to the reciprocity gap principle,  $\mathcal{G}$  would vanish identically if no inclusion or crack were present. Therefore it can be expected that the functional  $\mathcal{G}$  contains information on the unknown boundary or crack. We will use the identities (1.8) and (1.9) to derive two-by-two systems of integral equations for the pair of unknowns  $(\Gamma_0, p)$  and  $(\Gamma_c, h)$ , respectively, by choosing the test functions  $U$  as fundamental solutions  $\Phi$  with appropriately located sources. To obtain the equations for  $(\Gamma_0, p)$  we choose one set of functions with source points in  $D_1$  and another set with source points in  $D_0$ . Then the integral equations are derived from letting the source points tend to  $\Gamma_1$  and  $\Gamma_0$ , respectively. Analogously, for determining the equations for  $(\Gamma_c, h)$  one set of functions is chosen with source points in  $D_1$  and another set with

source points on  $\Gamma_c$ . We will show that solving the inverse problems is equivalent to solving the two-by-two systems of integral equations.

The integral equations are linear with respect to the densities  $p$  and  $h$  and nonlinear with respect to the boundary shapes  $\Gamma_0$  and  $\Gamma_c$ . For each of the two systems the equation resulting from the source points in  $D_1$  is severely ill-posed whereas the second equation is only mildly ill-posed. For the practical solution of the integral equations we propose a Newton iteration via linearization of the full two-by-two systems. Clearly, the ill-posedness requires to incorporate a regularization within each step of the Newton iterations. As in [20] we confine ourselves to the well-established Tikhonov regularization.

A standard approach to solving the above inverse problems is to apply Newton iterations to the nonlinear operator equations  $F_i(\Gamma_0) = g$  or  $F_c(\Gamma_c) = g$ , where for a fixed  $f$  the operators  $F_i$  and  $F_c$ , respectively, map the interior boundary  $\Gamma_0$  and  $\Gamma_c$  onto the normal derivative  $\partial u / \partial \nu|_{\Gamma_1}$  of the solution  $u$  to the boundary value problems (1.1)–(1.2) and (1.3)–(1.4), respectively. As opposed to this approach, our method does not require the solution of the forward problem in each iteration step, and the derivatives occurring in the linearization can be explicitly expressed in terms of integral operators rather than through associated boundary value problems. Both these properties lead to a noticeable reduction of the computational costs without diminishing the quality of the reconstructions.

Since the equations are linear with respect to the densities, one might also consider a second variant of Newton iterations. For the perfectly insulating inclusion, given a current approximation for  $\Gamma_0$ , one can first solve the severely ill-posed linear equation for the density  $p$  and then, keeping  $p$  fixed, linearize the second equation to update  $\Gamma_0$ . The same approach could also be pursued for the case of the perfectly conducting crack. However, we refrain from further pursuing this idea since the numerical experience as reported in [20] indicates that, for the perfectly conducting inclusion, this second variant leads to less accurate reconstructions than the full linearization.

The plan of the paper is as follows. In Section 2 we will derive the integral equations and prove their equivalence to the inverse problems. This is followed by the parameterization of the integral operators and their derivatives with respect to  $\Gamma_0$  and  $\Gamma_c$  in Section 3. After describing

the linearization and the iteration scheme in Section 4, we conclude with numerical examples in Section 5.

## 2. Nonlinear integral equations.

**2.1 Insulating inclusion.** In terms of the fundamental solution (1.11), we introduce double-layer potential operators

$$Q_j : L^2(\Gamma_0) \longrightarrow L^2(\Gamma_j), \quad j = 0, 1,$$

defined by

$$(2.1) \quad (Q_j p)(x) := - \int_{\Gamma_0} p(y) \frac{\partial \Phi(x, y)}{\partial \nu(y)} ds(y) - \frac{1-j}{2} p(x), \quad x \in \Gamma_j.$$

Note that  $Q_0$  contains the residual term for the limit of the double-layer potential when approaching  $\Gamma_0$  from inside  $D_0$ . In terms of the given functions  $f$  and  $g$ , we define the combined single- and double-layer potential

$$(2.2) \quad w(x) := \int_{\Gamma_1} \left\{ f(y) \frac{\partial \Phi(x, y)}{\partial \nu(y)} - g(y) \Phi(x, y) \right\} ds(y), \quad x \in \mathbf{R}^2 \setminus \Gamma_1.$$

Further, in terms of the unknown function  $p$ , we introduce the double-layer potential

$$(2.3) \quad v(x) := \int_{\Gamma_0} p(y) \frac{\partial \Phi(x, y)}{\partial \nu(y)} ds(y), \quad x \in \mathbf{R}^2 \setminus \Gamma_0.$$

Now we are in a position to state the following theorem.

**Theorem 2.1.** *The inverse boundary value problem for the perfect insulator and the system of integral equations*

$$(2.4) \quad Q_0 p = w|_{\Gamma_0}$$

and

$$(2.5) \quad Q_1 p = w|_{\Gamma_1}$$

are equivalent.

*Proof.* Let  $\Gamma_0$  be a solution to the inverse boundary value problem and  $p$  the corresponding Dirichlet data on  $\Gamma_0$ . Then, from (1.8) applied to  $U = \Phi(x, \cdot)$  with source point  $x \in \mathbf{R}^2 \setminus \overline{D}$ , we have

$$-v = w \quad \text{in } \mathbf{R}^2 \setminus \overline{D}.$$

By using the jump relations for single- and double-layer potentials, we observe that  $\Gamma_0$  and  $p$  satisfy the equations (2.4) and (2.5).

Conversely, if  $\Gamma_0$  and  $p$  satisfy (2.4) and (2.5), in view of the condition (1.6), the function  $w + v$  is bounded and harmonic in  $D_1$ . From (2.5) it follows that  $v + w = 0$  on  $\Gamma_1$ , hence  $v + w = 0$  in  $D_1$  by the uniqueness for the exterior Dirichlet problem for the Laplace equation. From (2.4) we conclude that  $v + w$  is harmonic in  $D_0$  and satisfies  $v + w = 0$  on  $\Gamma_0$ . Therefore, by the uniqueness for the interior Dirichlet problem, we have that  $v + w = 0$  in  $D_0$ . Now we define a harmonic function  $u := -v - w$  in  $D$ . Then from the jump relations for single- and double-layer potentials applied to  $v$  and  $w$ , we conclude that  $u = f$ ,  $\partial u / \partial \nu = g$  on  $\Gamma_1$  and  $u = p$ ,  $\partial u / \partial \nu = 0$  on  $\Gamma_0$ .  $\square$

We note that the integral equations (2.4) and (2.5) exploit (1.8) completely, since the set  $\{\Phi(x, \cdot) : x \in \mathbf{R}^2 \setminus \overline{D}\}$  is complete in  $W := \{U \in H^1(D) : \Delta U = 0 \text{ in } D\}$ , see [20].

**2.2 Perfectly conducting crack.** To derive nonlinear integral equations from (1.9), we introduce the single-layer operators

$$S_j : L^2(\Gamma_c) \longrightarrow L^2(\Gamma_j), \quad j = c, 1,$$

defined by

$$(2.6) \quad (S_j h)(x) := \int_{\Gamma_c} h(y) \Phi(x, y) ds(y), \quad x \in \Gamma_j.$$

As in the case of a perfectly conducting inclusion with closed boundary curve, see [20], in order to ensure boundedness at infinity for the operator  $S_1$  and the combined potential  $w$  as defined in (2.2), we introduce modifications  $\tilde{S}_1$  and  $\tilde{w}$  by

$$(2.7) \quad (\tilde{S}_1 h)(x) := (S_1 h)(x) + [1 - \Phi(x, 0)] \int_{\Gamma_c} h(y) ds(y), \quad x \in \Gamma_1,$$

and

$$(2.8) \quad \begin{aligned} \tilde{w}(x) &:= w(x) - [1 - \Phi(x, 0)] \int_{\Gamma_1} g(y) ds(y), \\ x &\in \mathbf{R}^2 \setminus \{\Gamma_1 \cup \{0\}\}. \end{aligned}$$

Here, without loss of generality, we assume that the origin is contained in  $D$ . After these definitions from (1.9), we can state the following theorem.

**Theorem 2.2.** *The inverse boundary value problem for the crack and the system of integral equations*

$$(2.9) \quad S_c h = w|_{\Gamma_c}$$

and

$$(2.10) \quad \tilde{S}_1 h = \tilde{w}|_{\Gamma_1}$$

are equivalent.

*Proof.* The proof is analogous to that for the case of a perfectly conducting inclusion as provided in [20].  $\square$

Note that (2.4) is a well-posed integral equation of the second kind and that equation (2.9) is only mildly ill-posed due to its singular kernel. However the equations (2.5) and (2.10) have smooth kernels and therefore their inversion is severely ill-posed.

### 3. Parameterized integral operators and derivatives.

**3.1 Inclusion reconstruction.** We assume that the boundary curves are parameterized in the form

$$\Gamma_j = \{z_j(t) : t \in [0, 2\pi]\}, \quad j = 0, 1,$$

where  $z_j : \mathbf{R} \rightarrow \mathbf{R}^2$  are  $2\pi$  periodic, twice continuously differentiable and injective functions. The latter property, in particular, implies

$z'_j(t) \neq 0$  for all  $t \in [0, 2\pi]$ . Furthermore, we assume that the orientations of  $\Gamma_j$ ,  $j = 0, 1$ , are counter-clockwise. For convenience, we introduce the vectors

$$\mu_j(\tau) = (-1)^j (-z'_{j,2}, z'_{j,1}), \quad j = 0, 1,$$

that are exterior normal vectors to  $\Gamma_j$ ,  $j = 0, 1$ . For simplicity we consider only starlike interior boundary curves with parameterization

$$(3.1) \quad z_0(t) = r(t)(\cos t, \sin t).$$

Here  $r : \mathbf{R} \rightarrow (0, \infty)$  is a  $2\pi$  periodic twice continuously differentiable function representing the radial distance from the origin. Then, setting  $\varphi = p \circ z_0$  and  $A_j\varphi = (Q_j(\varphi \circ z_0^{-1})) \circ z_j$ , we transform (2.1) into the parametric form

$$(A_j\varphi)(t) = -\frac{1}{2\pi} \int_0^{2\pi} \varphi(\tau) \frac{\mu_0(\tau) \cdot [z_j(t) - z_0(\tau)]}{|z_j(t) - z_0(\tau)|^2} d\tau - \frac{1-j}{2} \varphi(t),$$

$$t \in [0, 2\pi], \quad j = 0, 1.$$

The kernels of the parameterized double-layer potential operators  $A_j$  are smooth with the diagonal values for  $A_0$  given through the limit

$$(3.2) \quad \lim_{\tau \rightarrow t} \frac{\mu_j(\tau) \cdot [z_j(t) - z_j(\tau)]}{|z_j(t) - z_j(\tau)|^2} = \frac{\mu_j(t) \cdot z_j''(t)}{2|z_j^w(t)|^2}, \quad j = 0, 1,$$

for  $j = 0$ . For the parameterized form of the combined single- and double-layer potential  $w_j = w \circ z_j$  evaluated on  $\Gamma_j$ ,  $j = 0, 1$ , due to the jump relations, we have

$$(3.3) \quad w_j(t) = \frac{1}{2\pi} \int_0^{2\pi} f(z_1(\tau)) \frac{\mu_1(\tau) \cdot [z_j(t) - z_1(\tau)]}{|z_j(t) - z_1(\tau)|^2} d\tau + \frac{j}{2} f(z_1(t))$$

$$- \frac{1}{2\pi} \int_0^{2\pi} g(z_1(\tau)) \Phi(z_j(t), z_1(\tau)) |z_1'(\tau)| d\tau, \quad t \in [0, 2\pi].$$

We will use the notations  $w_0(r)$  and  $A_j(r, \varphi)$ ,  $j = 0, 1$ , to indicate the dependence on  $r$ . Note that  $w_1$  does not depend on  $r$ . Again, the kernel of  $w_0$  is smooth. In the kernel of  $w_1$ , the term arising from the

double-layer potential is smooth with diagonal values given by (3.2) for  $j = 1$  and the term stemming from the single-layer potential has a logarithmic singularity. For the numerical approximation of the latter, we note the decomposition

$$2\pi\Phi(z_1(t), z_1(\tau)) = -\ln \left| \sin \frac{t - \tau}{2} \right| + \ln \frac{|\sin(t - \tau/2)|}{|z_1(t) - z_1(\tau)|},$$

where the second term is smooth with diagonal values

$$\lim_{\tau \rightarrow t} \ln \frac{|\sin(t - \tau/2)|}{|z_1(t) - z_1(\tau)|} = -\ln 2|z_1'(t)|.$$

Hence, the well-established quadrature rules for  $2\pi$  periodic logarithmic singularities as described in [18] are available. For the  $2\pi$  periodic smooth kernels in all the operators, of course, the trapezoidal rule can be employed for the numerical approximation.

With these notations, the integral equations (2.4) and (2.5) are transformed into

$$(3.4) \quad A_0(r, \varphi) = w_0(r)$$

and

$$(3.5) \quad A_1(r, \varphi) = w_1.$$

For solving these nonlinear equations via Newton iterations, the derivatives of the operators  $A_j$  and the potential  $w_0$  with respect to the interior boundary  $\Gamma_0$  are required. The Fréchet derivatives of these operators can be obtained by formally differentiating their kernels with respect to  $r$ , see [24]. Hence, the derivative of  $A_0$  in direction  $q$  is given by

$$\begin{aligned} & A_0'(r, \varphi; q)(t) \\ &= \frac{1}{\pi} \int_0^{2\pi} \varphi(\tau) \frac{\mu_0(\tau) \cdot [z_0(t) - z_0(\tau)] [z_0(t) - z_0(\tau)] \cdot [\zeta_0(t) - \zeta_0(\tau)]}{|z_0(t) - z_0(\tau)|^4} d\tau \\ &\quad - \frac{1}{2\pi} \int_0^{2\pi} \varphi(\tau) \frac{\mu_0(\tau) \cdot [\zeta_0(t) - \zeta_0(\tau)] + [\zeta_0'(\tau)]^\perp \cdot [z_0(t) - z_0(\tau)]}{|z_0(t) - z_0(\tau)|^2} d\tau \end{aligned}$$

for  $t \in [0, 2\pi]$ . Here, we have set  $\zeta_0(t) = q(t)(\cos t, \sin t)$  and

$$[\zeta'_0(t)]^\perp = q'(t)(-\sin t, \cos t) - q(t)(\cos t, \sin t).$$

The kernel  $H(t, \tau)$  of the integral operator  $A'_0$  is smooth with the diagonal values

$$\tilde{H}(t) := \lim_{t \rightarrow \tau} H(t, \tau)$$

given by

$$\tilde{H} = \frac{q''(rr'^2 + r^3) - 2q'(rr'r'' + r'r^2) + q(2rr'^2 - r^2r'' + r''r'^2)}{2(r'^2 + r^2)^2}.$$

Analogously, the Fréchet derivatives of the operator  $A_1$  and the potential  $w_0$  are given by

$$\begin{aligned} & A'_1(r, \varphi; q)(t) \\ &= \frac{1}{\pi} \int_0^{2\pi} \varphi(\tau) \frac{\mu_0(\tau) \cdot [z_1(t) - z_0(\tau)] [z_1(t) - z_0(\tau)] \cdot \zeta_0(\tau)}{|z_1(t) - z_0(\tau)|^4} d\tau \\ &+ \frac{1}{2\pi} \int_0^{2\pi} \varphi(\tau) \frac{[\zeta'_0(\tau)]^\perp \cdot [z_1(t) - z_0(\tau)] - \mu_0(\tau) \cdot \zeta_0(\tau)}{|z_0(t) - z_0(\tau)|^2} d\tau, \\ & t \in [0, 2\pi], \end{aligned}$$

and

$$\begin{aligned} (3.6) \quad & w'_0(r; q)(t) \\ &= -\frac{1}{\pi} \int_0^{2\pi} f(z_1(\tau)) \frac{\mu_1(\tau) \cdot [z_0(t) - z_1(\tau)] [z_0(t) - z_1(\tau)] \cdot \zeta_0(t)}{|z_0(t) - z_1(\tau)|^4} d\tau \\ &+ \frac{1}{2\pi} \int_0^{2\pi} f(z_1(\tau)) \frac{\mu_1(\tau) \cdot \zeta_0(t)}{|z_0(t) - z_1(\tau)|^2} d\tau \\ &+ \frac{1}{2\pi} \int_0^{2\pi} g(z_1(\tau)) \frac{[z_0(t) - z_1(\tau)] \cdot \zeta_0(t)}{|z_0(t) - z_1(\tau)|^2} |z'_1(\tau)| d\tau, \\ & t \in [0, 2\pi]. \end{aligned}$$

The operators  $A'_1$  and  $w'_0$  both have smooth kernels and, of course,  $w'_0(q) = \zeta_0 \cdot (\text{grad } w) \circ z_0$ .

**3.2 Crack reconstruction.** We assume that the crack  $\Gamma_c \subset \mathbf{R}^2$  is an open curve of class  $C^3$ , i.e.,

$$(3.7) \quad \Gamma_c = \{\sigma(s) : s \in [-1, 1]\},$$

where  $\sigma : [-1, 1] \rightarrow \mathbf{R}^2$  is three times continuously differentiable and injective. The latter property ensures that  $\sigma'(s) \neq 0$  for all  $s \in [-1, 1]$ . To incorporate the square root singularities of the solution  $u$  at the crack tips, see [13], we apply the cosine transformation as suggested by Yan and Sloan [25]. We substitute  $s = \cos t$  for  $t \in [0, \pi]$  into the presentation (3.7) and transform the integral operator (2.6) into the parametric form

$$(3.8) \quad (B_c \varphi)(t) = \int_0^\pi \varphi(\tau) \Phi(z_c(t), z_c(\tau)) d\tau, \quad t \in [0, \pi].$$

Here we have set

$$z_c(t) := \sigma(\cos t), \quad t \in [0, \pi],$$

and

$$\varphi(t) := |\sin t| |\sigma'(\cos t)| h(z_c(t)), \quad t \in [0, \pi].$$

Since the integrand in (3.8) can be considered as an even  $2\pi$  periodic function, we can rewrite it in the form

$$(3.9) \quad (B_c \varphi)(t) = \frac{1}{2} \int_0^{2\pi} \varphi(\tau) \Phi(z_c(t), z_c(\tau)) d\tau, \quad t \in [0, \pi].$$

To cope with the logarithmic singularity of the kernel we proceed as in [16] and split

$$2\pi \Phi(z_c(t), z_c(\tau)) = -\ln \left( \frac{1}{2} |\cos t - \cos \tau| \right) + H(t, \tau)$$

where

$$H(t, \tau) := \ln \frac{|\cos t - \cos \tau|}{2 |z_c(t) - z_c(\tau)|}$$

is smooth with diagonal values

$$\lim_{\tau \rightarrow t} H(t, \tau) = -\ln 2 |z_c'(t)|.$$

From the identity

$$(3.10) \quad \ln \left( \frac{1}{2} |\cos t - \cos \tau| \right) = \ln \left| \sin \frac{t - \tau}{2} \right| + \ln \left| \sin \frac{t + \tau}{2} \right|,$$

substituting  $\tau$  by  $-\tau$  in (3.9) for the integral corresponding to the second term on the right side of (3.10) it can be seen that

$$(3.11) \quad (B_c \varphi)(t) = \frac{1}{2\pi} \int_0^{2\pi} \left\{ -\ln \left| \sin \frac{t - \tau}{2} \right| + \frac{1}{2} H(t, \tau) \right\} \varphi(\tau) d\tau, \\ t \in [0, \pi].$$

Hence, the logarithmic singularity is of the same type as for the single-layer potential part of  $w_1$  over the closed curve  $\Gamma_1$  from the previous subsection and therefore the same quadratures can be applied.

For the operator  $\tilde{S}_1$  as defined by (2.10) the cosine substitution leads to

$$(\tilde{B}_1 \varphi)(t) = \int_0^\pi \varphi(\tau) \Phi(z_1(t), z_c(\tau)) d\tau + [1 - \Phi(z_1(t), 0)] \int_0^\pi \varphi(\tau) d\tau, \\ t \in [0, 2\pi].$$

For the numerical approximation of the operator  $\tilde{B}_1$  with smooth kernel we again use the fact that the integrand can be smoothly extended as a  $2\pi$  periodic even function and apply the trapezoidal rule.

Analogous to the previous subsection, the parameterization of the potential  $w$  on  $\Gamma_c$  yields

$$w_c(t) = \frac{1}{2\pi} \int_0^{2\pi} f(z_1(\tau)) \frac{\mu_1(\tau) \cdot [z_c(t) - z_1(\tau)]}{|z_c(t) - z_1(\tau)|^2} d\tau \\ - \frac{1}{2\pi} \int_0^{2\pi} g(z_1(\tau)) \Phi(z_c(t), z_1(\tau)) |z_1'(\tau)| d\tau, \quad t \in [0, \pi],$$

where  $w_c := w \circ z_c$ . The parameterization  $\tilde{w}_1 = \tilde{w} \circ z_1$  of the modified potential  $\tilde{w}$  on  $\Gamma_1$  is given by

$$\tilde{w}_1(t) = w_1(t) - [1 - \Phi(z_1(t), 0)] \int_0^{2\pi} g(\tau) d\tau, \quad t \in [0, 2\pi],$$

with  $w_1$  as in (3.3).

As in the previous subsection we will use the notations  $w_c(z_c)$ ,  $B_c(z_c, \varphi)$ ,  $\tilde{B}_1(z_c, \varphi)$  to indicate the dependence of the crack parameterized by  $z_c$ . With the above notations, the integral equations (2.9) and (2.10) can now be rewritten in the parametric form

$$(3.12) \quad B_c(z_c, \varphi) = w_c(z_c)$$

and

$$(3.13) \quad \tilde{B}_1(z_c, \varphi) = \tilde{w}_1.$$

The Fréchet derivatives at  $z_c$  in the direction  $\zeta_c$  are given by

$$(3.14) \quad B'_c(z_c, \varphi; \zeta_c)(t) = -\frac{1}{2\pi} \int_0^\pi \varphi(\tau) \frac{[z_c(t) - z_c(\tau)] \cdot [\zeta_c(t) - \zeta_c(\tau)]}{|z_c(t) - z_c(\tau)|^2} d\tau, \\ t \in [0, \pi].$$

Here, as for  $z_c(t) = \sigma(\cos t)$  we have substituted  $\zeta_c(t) = \sigma_\zeta(\cos t)$  for some  $\sigma_\zeta$  creating a perturbed crack with parameterization  $\sigma + \sigma_\zeta$ . The kernel in (3.14) is smooth with diagonal values

$$\lim_{\tau \rightarrow t} \frac{[z_c(t) - z_c(\tau)] \cdot [\zeta_c(t) - \zeta_c(\tau)]}{|z_c(t) - z_c(\tau)|^2} = \frac{z'_c(t) \cdot \zeta'_c(t)}{|z'_c(t)|^2}.$$

Finally, the derivative of the operator  $\tilde{B}_1$  is given by

$$\tilde{B}'_1(z_c, \varphi; \zeta_c)(t) = \frac{1}{2\pi} \int_0^\pi \varphi(\tau) \frac{[z_c(t) - z_c(\tau)] \cdot \zeta_c(\tau)}{|z_c(t) - z_c(\tau)|^2} d\tau, \quad t \in [0, 2\pi],$$

and for the Fréchet derivative  $w'_c(z_c; \zeta_c)$  we have the same formula as for  $w'_0(r; q)$  in (3.6) with  $z_0$  and  $\zeta_0$  replaced by  $z_c$  and  $\zeta_c$ , respectively, and for  $t \in [0, \pi]$ .

**4. The iteration scheme.** Since the integral operators  $A_0$  and  $A_1$  are linear with respect to  $\varphi$ , the linearization of the system (3.4)–(3.5) leads to

$$(4.1) \quad A_0(r, \varphi) + A_0(r, \psi) + A'_0(r, \varphi; q) = w_0(r) + w'_0(r; q)$$

and

$$(4.2) \quad A_1(r, \varphi) + A_1(r, \psi) + A_1'(r, \varphi; q) = w_1.$$

Given a current approximation for  $r$  and  $\varphi$ , the linear system (4.1) and (4.2) needs to be solved for  $q$  and  $\psi$  to obtain the update  $r + q$  for the radial function and  $\varphi + \psi$  for the boundary values. Then, in an obvious way, this procedure is iterated. Clearly, the ill-posedness requires to incorporate a regularization in order to achieve stability. For this, in our numerical examples we used the well-established Tikhonov regularization with a Sobolev penalty term on the radial function and an  $L^2$  penalty term on the boundary values.

Analogously, the linearization of (3.12)–(3.13) yields

$$(4.3) \quad B_c(z_c, \varphi) + B_c(z_c, \psi) + B_c'(z_c, \varphi; \zeta_c) = w_c(z_c) + w_c'(z_c; \zeta_c)$$

and

$$(4.4) \quad \tilde{B}_1(z_c, \varphi) + \tilde{B}_1(z_c, \psi) + \tilde{B}_1'(z_c, \varphi; \zeta_c) = \tilde{w}_1.$$

The following theorem claims the injectivity of the linearization (4.1)–(4.2) at the exact solution.

**Theorem 4.1.** *Let  $r$  be the parameterization of the interior boundary  $\Gamma_0$  and let  $\varphi = u \circ z_0$  in terms of the solution  $u$  of (1.1)–(1.2). Assume that  $q \in C^2[0, 2\pi]$  and  $\psi \in L^2[0, 2\pi]$  solve the homogeneous system*

$$(4.5) \quad A_0(r, \psi) + A_0'(r, \varphi; q) - w_0'(r; q) = 0$$

and

$$(4.6) \quad A_1(r, \psi) + A_1'(r, \varphi; q) = 0.$$

Then  $q = 0$  and  $\psi = 0$ .

*Proof.* We begin by showing that, for sufficiently small  $q$ , the perturbed interior curve as given in polar coordinates by

$$\Gamma_{r+q} = \{(r(t) + q(t))(\cos t, \sin t) : t \in [0, 2\pi]\}$$

can be represented in the form

$$\Gamma_{r+q} = \{r(t)(\cos t, \sin t) + \tilde{q}(t)\nu(t) : t \in [0, 2\pi]\}$$

in terms of the unit normal vector

$$\nu(t) = r'(t)(-\sin t, \cos t) - r(t)(\cos t, \sin t)$$

to the unperturbed curve  $\Gamma_r = \Gamma_0$  and a function  $\tilde{q}$ . For this we need to show that each point  $y$  in some neighborhood of  $\Gamma_0$  can be represented in the form

$$y = r(t)(\cos t, \sin t) + \eta\nu(t)$$

for some  $t \in [0, 2\pi]$  and some  $\eta \in \mathbf{R}$ . To this end, for sufficiently small  $h > 0$ , we consider the corresponding map  $F : [0, 2\pi] \times [-h, h] \rightarrow \mathbf{R}^2$  given by

$$F(t, \eta) = r(t)(\cos t, \sin t) + \eta\nu(t).$$

Since

$$\frac{\partial F}{\partial t}(t, 0) = r'(t)(\cos t, \sin t) + r(t)(-\sin t, \cos t) \quad \text{and} \quad \frac{\partial F}{\partial \eta}(t, 0) = \nu(t),$$

obviously, for sufficiently small  $h$  the mapping  $F$  is bijective. From the analysis in Subsection 3.1 we observe that in the Fréchet derivatives  $A'_0, A'_1$  and  $w'_0$  we now may replace the perturbation vector  $\zeta_0(t) = q(t)(\cos t, \sin t)$  by  $\tilde{\zeta}_0 = \tilde{q}\nu$ .

We introduce the function

$$\begin{aligned} V(x) := & \int_0^{2\pi} \psi(\tau) \operatorname{grad}_x \Phi(x, z_0(\tau)) \cdot \nu(z_0(\tau)) d\tau \\ & + \int_0^{2\pi} \varphi(\tau) \operatorname{grad}_x (\operatorname{grad}_x \Phi(x, z_0(\tau)) \cdot \nu(z_0(\tau))) \cdot \tilde{\zeta}_0(\tau) d\tau, \\ & x \in \mathbf{R}^2 \setminus \Gamma_0. \end{aligned}$$

Then (4.6) implies that  $V = 0$  on  $\Gamma_1$ . Since  $V$  is bounded in  $D_1$ , from the uniqueness for the exterior Dirichlet problem and analyticity we can conclude that  $V = 0$  in  $D \cup \overline{D}_1$ .

In view of the jump relations from equation (4.5) and  $V = 0$  in  $D$ , by approaching  $\Gamma_0$  from inside  $D$  we conclude that

$$\psi + \tilde{\zeta}_0 \cdot (\text{grad}[v + w]) \circ z_0 = 0,$$

that is,

$$(4.7) \quad \psi + \tilde{q} \nu \cdot (\text{grad}[v + w]) \circ z_0 = 0.$$

Recalling from the proof of Theorem 2.1 that  $u = -v - w$  in  $D$  and using  $\partial u / \partial \nu = 0$  on  $\Gamma_0$ , from (4.7) we now obtain that  $\psi = 0$ . Therefore the property  $V = 0$  in  $D$  simplifies into

$$\int_0^{2\pi} \tilde{\varphi}(\tau) \text{grad}_x(\text{grad}_x \Phi(x, z_0(\tau)) \cdot \nu(z_0(\tau))) \cdot \nu(z_0(\tau)) d\tau = 0, \quad x \in D,$$

where we have set  $\tilde{\varphi} := \varphi \tilde{q}$ . Note that  $\tilde{\varphi}$  is continuous. Working out the derivatives, and making use of periodicity, we rewrite this into the form

$$(4.8) \quad V_1(x) + V_2(x) = 0, \quad x \in D,$$

for

$$V_1(x) := -2 \int_{-\pi}^{\pi} \tilde{\varphi}(\tau) \frac{[(x - z_0(\tau)) \cdot \nu(z_0(\tau))]^2}{|x - z_0(\tau)|^4} d\tau$$

and

$$V_2(x) := \int_{-\pi}^{\pi} \frac{\tilde{\varphi}(\tau)}{|x - z_0(\tau)|^2} d\tau.$$

The kernel in the integral for  $V_1$  coincides with the square of the kernel of the double-layer potential. Therefore, proceeding as in the proof for the jump relations of the double-layer potential (see the proof of Theorem 6.17 in [18]) it can be seen that the function  $V_1$  is bounded in  $D$ . Consequently, in view of (4.8), the function  $V_2$  also must be bounded in  $D$ .

Now assume that  $\tilde{\varphi} \neq 0$ . Then, because  $\tilde{\varphi}$  is continuous, without loss of generality we may assume that there exist positive numbers

$\delta$  and  $\mu$  with  $\delta < \pi$  such that  $\tilde{\varphi}(\tau) \geq \mu$  for  $|\tau| \leq \delta$ . Then for  $x = z_0(0) + h\nu(z_0(0))$  we can estimate

$$|z_0(\tau) - x|^2 \leq 2|z_0(\tau) - z_0(0)|^2 + 2h^2 \leq 2\|z_0'\|_\infty \tau^2 + 2h^2 \leq C(\tau^2 + h^2)$$

for all  $|\tau| \leq \delta$  and some constant  $C > 0$ . Consequently we can estimate

$$(4.9) \quad \int_{-\delta}^{\delta} \frac{\tilde{\varphi}(\tau)}{|x - z_0(\tau)|^2} d\tau \geq \frac{\mu}{C} \int_{-\delta}^{\delta} \frac{1}{\tau^2 + h^2} d\tau = \frac{2\mu}{Ch} \arctan \frac{\delta}{h}.$$

Since the remaining integral over  $\delta \leq |\tau| \leq \pi$  in the expression for  $V_2(x)$ , for sufficiently small  $h$ , is uniformly bounded with respect to  $h$ , from (4.9) we conclude that

$$\lim_{h \rightarrow 0} V_2(z_0(0) + h\nu(z_0(0))) = \infty,$$

which is a contradiction to the boundedness of  $V_2$  in  $D$ . Hence,  $\tilde{\varphi} = 0$  and consequently  $\varphi \tilde{q} = 0$ . From Holmgren's theorem and the homogeneous Neumann boundary condition for  $u$  on  $\Gamma_0$ , we conclude that  $u$  cannot vanish on an open subset of  $\Gamma_0$ . Therefore, in view of  $\varphi = u \circ z_0$ , we finally conclude that  $\tilde{q} = 0$  and consequently  $q = 0$  and this concludes the proof.  $\square$

A corresponding result for the perfectly conducting crack can be shown analogously to the case of a perfectly conducting inclusion in [20]. We note that the proof of Theorem 4.1 required additional techniques as compared with that of Theorem 5.1 in [20].

**5. Numerical examples.** In this final section we present some numerical results for the reconstruction method described above both for the perfectly insulating inclusion and the perfectly conducting crack. For the sake of simplicity, in all examples, the outer boundary  $\Gamma_1$  is chosen to be the unit circle, i.e.,  $z_1(t) = (\cos t, \sin t)$ . The synthetic data  $g$  were obtained by solving the direct problem (1.1)–(1.2) for the inclusion and (1.3)–(1.4) for the crack by the Green's function approach as described in [11]. Roughly speaking, this approach solves both problems by a superposition of the solution for the Dirichlet problem for the unit disk and a single-layer potential with an unknown density on  $\Gamma_0$

and  $\Gamma_c$ , respectively, and with the Green's function for the unit disk as kernel. In the case of the Neumann boundary condition, this leads to a boundary integral equation of the second kind on the boundary  $\Gamma_0$  that can be numerically solved by the Nyström method. In the case of the Dirichlet condition on the crack  $\Gamma_c$  the resulting integral equation is of the first kind and can be solved via the cosine transformation. In order to compute the normal derivative on  $\Gamma_1$  it is required to evaluate the normal derivative of the Poisson integral which leads to a hypersingular integral. To deal with this singularity we use Garrick's quadrature formula and trigonometric interpolation as described in [17].

Using the Green's function approach for creating the synthetic data clearly avoids committing an inverse crime, since the inverse solver is not based on using the Green's function. For noisy data, random errors are added pointwise to  $g$  with the percentage given in terms of the  $L^2$  norm. In all examples the regularization parameters were chosen by trial and error.

We begin with considering the numerical solution of the inverse boundary value problem (1.1), (1.2) and (1.5), i.e., the reconstruction of an inclusion. Here, we assume that the interior boundary is starlike, i.e., that it is given in the form (3.1). As finite dimensional space for the approximation and the update we use the space of trigonometric polynomials of degree less than or equal to  $K$ , that is,

$$(5.1) \quad q(t) = \sum_{m=0}^K a_m \cos mt + \sum_{m=1}^K b_m \sin mt.$$

To approximate the integral operators in (4.1)–(4.2) we use  $2M$  equidistant quadrature points for the trapezoidal rule and the logarithmic singularity quadrature. Further, for the solution of the linear equations (4.1)–(4.2) we apply a fully discrete collocation at the same  $2M$  equidistant points to obtain a  $4M \times 4M$  linear system for the  $2K + 1$  coefficients  $(a_m, b_m)$  from (5.1) and the  $2M$  approximate values for  $\psi(t_0), \dots, \psi(t_{2M-1})$ , where  $t_j = \pi j/M$ ,  $j = 0, \dots, 2M - 1$ . Due to the ill-posedness, Tikhonov regularization is incorporated with a Sobolev  $H^l$  penalty term on  $q$  and  $L^2$  penalty term on  $\psi$ . The initial guess for the interior boundary  $\Gamma_0$  is chosen as a circle of radius 0.8 centered at the origin. We denote the regularization parameters for penalizing  $\psi$  and  $q$  by  $\alpha$  and  $\beta$ , respectively.

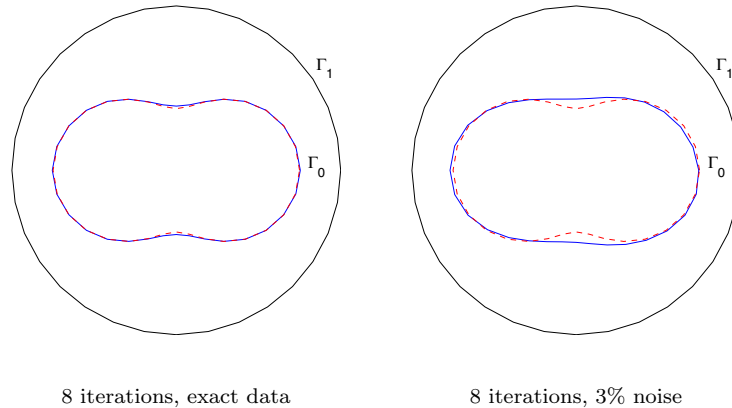


FIGURE 1. Reconstruction of a peanut-shaped contour.

In the first example, we consider the identification of a peanut shaped boundary curve  $\Gamma_0$  given by the radial function

$$r(t) = \frac{3}{4} \sqrt{\cos^2 t + 0.25 \sin^2 t}, \quad t \in [0, 2\pi].$$

The boundary data are of the form

$$f(z_1(t)) = \exp(-\cos^2 t), \quad t \in [0, 2\pi].$$

The reconstructions with  $M = 16$ ,  $K = 8$ ,  $\alpha = 1e - 9$ ,  $\beta = 1e - 7$ ,  $l = 2$  are presented in Figure 1. For the reconstruction with 3% random noise we choose the regularization parameters  $\alpha = 1e - 4$ ,  $\beta = 1e - 3$ , with the other parameters remaining unchanged. The correct interior boundary  $\Gamma_0$  is presented by the dashed line and the reconstruction by the solid line.

For the second example we consider the reconstruction of an apple-shaped contour with radial function

$$r(t) = \frac{0.5 + 0.4 \cos t + 0.1 \sin 2t}{1 + 0.7 \cos t}, \quad t \in [0, 2\pi].$$

The Dirichlet data are the same as in the first example. The results for  $\alpha = 1e - 6$ ,  $\beta = 1e - 4$ ,  $M = 16$ ,  $K = 6$ ,  $l = 0$  without noise and for  $\alpha = 0.0001$ ,  $\beta = 0.005$  with 3% noise are presented in Figure 2.

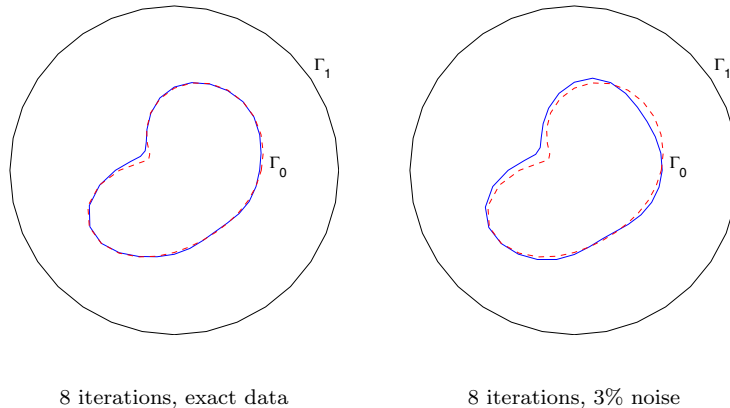


FIGURE 2. Reconstruction of an apple-shaped contour.

In the third example we consider a kite-shaped inclusion with the parameterization

$$z_0(t) = (0.6 \cos t + 0.3 \cos 2t - 0.2, 0.6 \sin t), \quad t \in [0, 2\pi]$$

and the Dirichlet data

$$f(z_1(t)) = \cos t + \sin t, \quad t \in [0, 2\pi].$$

The reconstruction with exact data for  $M = 24$ ,  $K = 16$ ,  $l = 2$ ,  $\alpha = 0.0001$ ,  $\beta = 0.001$  and with 3% noise are shown in Figure 3.

We conclude with some numerical examples for crack identification (compare also [21]). As finite dimensional space for the reconstructions and the updates  $\zeta_c$ , we choose the space of Chebyshev polynomials of degree less than or equal to  $K$ , that is,

$$(5.2) \quad \zeta_c(s) = \sum_{j=0}^K a_j T_j(s), \quad s \in [-1, 1],$$

with coefficients  $a_j \in \mathbf{R}^2$ . To approximate the integral operators in (4.3)–(4.4) we use  $2M$  equidistant quadrature points for the trapezoidal

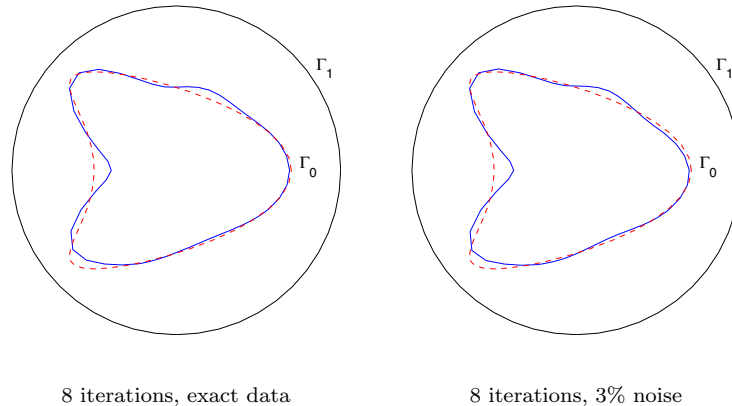


FIGURE 3. Reconstruction of a kite-shaped contour.

rule and the logarithmic singularity quadrature. Again, for the solution of the linear equations (4.3)–(4.4) we apply a fully discrete collocation at the same  $2M$  equidistant points to obtain a  $(3M + 1) \times (3M + 1)$  linear system for the  $2K + 2$  components of the coefficients  $a_j$  in (5.2) and the  $M + 1$  approximate values for  $\psi(t_0), \dots, \psi(t_M)$ . Here, the symmetry property  $\psi(t_j) = \psi(t_{2M-j})$  for  $t_j = 2\pi j/M$ ,  $j = 0, \dots, M$  is incorporated. Since the linearized equations inherit the ill-posedness from the equations (3.12)–(3.13), a Tikhonov regularization with an  $L_\omega^2$  penalty term with a weight  $\omega(s) = 1/\sqrt{1-s^2}$  is applied both for  $\zeta$  and  $\psi$ . We denote the regularization parameters for penalizing  $\psi$  and  $q$  by  $\alpha$  and  $\beta$ , respectively. As a stopping rule we use the condition

$$\frac{\|\zeta_c\|_{L_\omega^2[0,\pi]}}{\|z_c\|_{L_\omega^2[0,\pi]}} < \delta,$$

where  $\delta$  is a given tolerance. For all examples we choose the parameters  $M = 32$ ,  $K = 7$  and  $\delta = 0.0001$ .

We start by presenting the reconstruction of a parabolic crack given by

$$z(s) = (0.5s, 0.5(s^2 - 0.5)), \quad s \in [-1, 1].$$

The boundary data are of the form

$$(5.3) \quad f(z_1(t)) = 1 + \cos^2 t, \quad t \in [0, 2\pi].$$

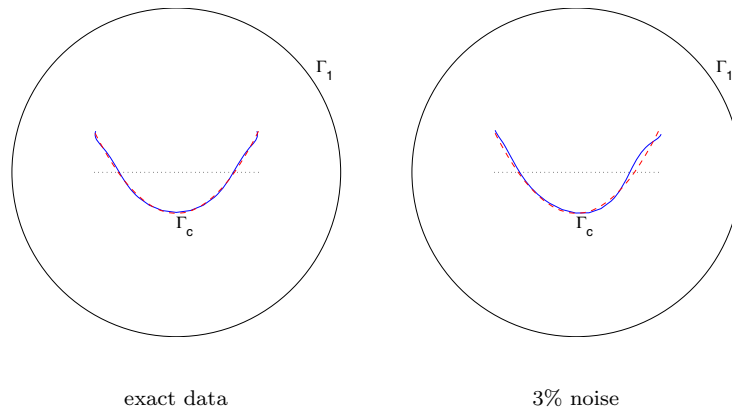


FIGURE 4. Reconstruction of a parabolic crack.

The initial guess for  $\Gamma_c$  is chosen as the straight line  $\{(0.5s, 0) : s \in [-1, 1]\}$ . The results with the parameters  $\alpha = 0.001$ ,  $\beta = 0.01$  and data without noise and with 3% noise are presented in Figure 4. The exact crack  $\Gamma_c$  is given by the dashed line, the reconstruction by the solid line and the initial guess by the dotted line.

In Figure 5 we show the reconstructions of a crack with the parameterization

$$(5.4) \quad z(s) = (0.5(s^2 + s - 1), 0.125(s^2 + 0.5s^4)), \quad s \in [-1, 1],$$

with Dirichlet data (5.3), the regularization parameters  $\alpha = 0.0001$ ,  $\beta = 0.001$  for exact data and  $\alpha = 0.001$ ,  $\beta = 0.01$  for data with 3% noise. The initial guess for  $\Gamma_c$  is chosen as  $\{(0.5s, -0.1) : s \in [-1, 1]\}$ .

In the last example, we present a reconstruction of a crack that is not contained in the approximation space, i.e., in the space of polynomials of degree less than or equal to  $K$ , and has the parameterization

$$(5.5) \quad z(s) = \frac{1}{2} \left( s, \sin \frac{3s}{2} \right), \quad s \in [-1, 1].$$

The Dirichlet data are given by

$$f(z_1(t)) = \exp(-\sin^2 t), \quad t \in [0, 2\pi].$$

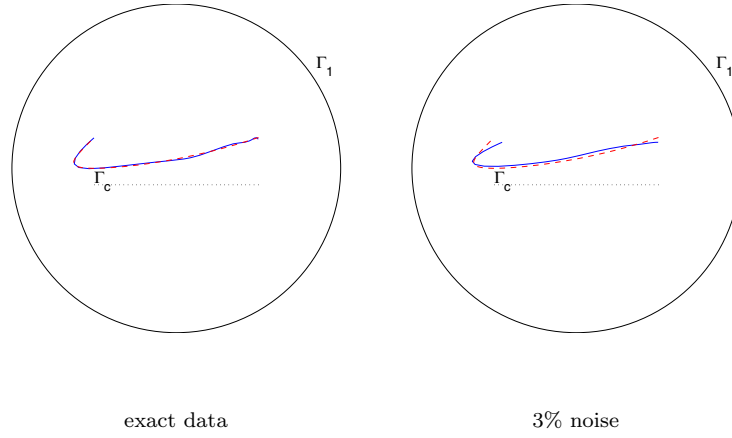


FIGURE 5. Reconstructions of the crack (5.4).

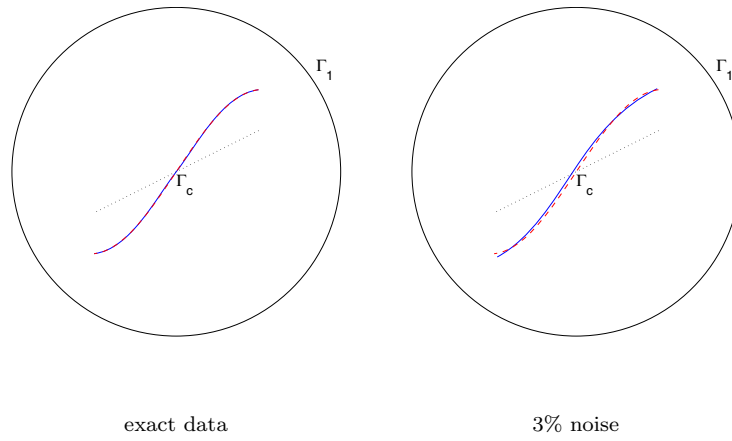


FIGURE 6. Reconstructions of the crack (5.5).

The initial guess for the crack  $\Gamma_c$  is chosen as  $\{(0.5s, 0.25s) : s \in [-1, 1]\}$ . The reconstruction for exact data and data with 3% noise with regularization parameters  $\alpha = 0.01$ ,  $\beta = 0.1$  are presented in Figure 6.

Summarizing, the numerical results show rather accurate reconstructions with reasonable stability against noisy data. In particular, the crack reconstructions show a satisfying identification of the location of the crack tips. Further numerical experiments indicated that for a noise level above about 5% the reconstructions started to deteriorate.

## REFERENCES

1. G. Alessandrini, *Stability for the crack determination problem*, in *Inverse problems in mathematical physics* (L. Päivärinta, et al., eds.), Springer-Verlag, Berlin, 1993, pp. 1–8.
2. G. Alessandrini, E. Beretta, E. Rosset and S. Vessella, *Optimal stability for inverse elliptic boundary value problems with unknown boundaries*, Ann. Scuola Norm. Sup. Pisa, Cl. Sci. IV. **29** (2000), 755–806.
3. G. Alessandrini, E. Beretta, F. Santosa and S. Vessella, *Stability in crack determination from electrostatic measurements at the boundary – A numerical investigation*, Inverse Problems **11** (1995), L17–L24.
4. G. Alessandrini, E. Beretta and S. Vessella, *Determining linear cracks by boundary measurements: Lipschitz stability*, SIAM J. Math. Anal. **27** (1996), 361–375.
5. G. Alessandrini and L. Rondi, *Optimal stability for the inverse problem of multiple cavities*, J. Differential Equations **176** (2001), 356–386.
6. S. Andrieux and A. Ben Abda, *Identification of planar crack by complete overdetermined data: Inversion formulae*, Inverse Problems **12** (1996), 553–563.
7. K.E. Atkinson, *The numerical solution of integral equations of the second kind*, Cambridge Univ. Press, Cambridge, 1997.
8. E. Beretta and S. Vessella, *Stable determination of boundaries from Cauchy data*, SIAM J. Math. Anal. **30** (1999), 220–232.
9. K. Bryan, F.R. Osborne, III and M. Vellela, *Reconstruction of cracks with unknown transmission condition from boundary data*, Inverse Problems **21** (2005), 21–36.
10. A.L. Bukhgeim, J. Cheng and M. Yamamoto, *Stability for an inverse boundary problem of determining a part of a boundary*, Inverse Problems **15** (1999), 1021–1032.
11. R. Chapko and R. Kress, *A hybrid method for inverse boundary value problems in potential theory*, J. Inverse Ill-Posed Probl. **13** (2005), 27–40.
12. J. Cheng, Y.C. Hon and M. Yamamoto, *Conditional stability for an inverse Neumann boundary problem*, Appl. Anal. **83** (2004), 49–62.
13. A. Friedman and M. Vogelius, *Determining cracks by boundary measurements*, Indiana Univ. Math. J. **38** (1989), 527–556.
14. R. González and R. Kress, *On the treatment of a Dirichlet-Neumann mixed boundary value problem for harmonic functions by an integral equations method*, SIAM J. Math. Anal. **8** (1977), 504–517.

15. H. Haddar and R. Kress, *Conformal mappings and inverse boundary value problems*, Inverse Problems **21** (2005), 935–953.
16. R. Kress, *Inverse scattering from an open arc*, Math. Meth. Appl. Sci. **18** (1995), 267–294.
17. ———, *On the numerical solution of a hypersingular integral equation in scattering theory*, J. Comp. Appl. Math. **61** (1995), 345–360.
18. ———, *Linear integral equations*, 2nd ed., Springer-Verlag, Heidelberg, 1999.
19. ———, *Inverse Dirichlet problem and conformal mapping*, Math. Comp. Simulation **66** (2004), 255–265.
20. R. Kress and W. Rundell, *Nonlinear integral equations and iterative solution for an inverse boundary value problem*, Inverse Problems **21** (2005), 1207–1223.
21. R. Kress and P. Serranho, *A hybrid method for two-dimensional crack reconstruction*, Inverse Problems **21** (2005), 773–784.
22. P.D. Lax and R.S. Phillips, *Scattering theory*, Academic Press, New York, 1967.
23. W. McLean, *Strongly elliptic systems and boundary integral equations*, Cambridge Univ. Press, Cambridge, 2000.
24. R. Potthast, *Fréchet differentiability of boundary integral operators in inverse acoustic scattering*, Inverse Problems **10** (1994), 431–447.
25. Y. Yan and I.H. Sloan, *On integral equations of the first kind with logarithmic kernels*, J. Integral Equations Appl. **1** (1988), 549–579.

INSTITUT FÜR NUMERISCHE UND ANGEWANDTE MATHEMATIK, UNIVERSITÄT  
GÖTTINGEN, 37083 GÖTTINGEN, GERMANY  
E-mail address: kress@math.uni-goettingen.de

INSTITUT FÜR NUMERISCHE UND ANGEWANDTE MATHEMATIK, UNIVERSITÄT  
GÖTTINGEN, 37083 GÖTTINGEN, GERMANY  
E-mail address: ivanyshy@math.uni-goettingen.de